Further Experimental Investigations of a Cesium Hall-Current Accelerator

CLYDE O. BROWN* AND EDWARD A. PINSLEY†
United Aircraft Corporation, East Hartford, Conn.

Analysis of an electrical propulsion thrustor employing Hall-current acceleration of cesium ions has shown that high thrust densities and efficiencies are achievable at moderate specific impulses (1500–5000 sec). Axial ion acceleration occurs within an annular, electrically neutral, cesium plasma; a radial magnetic field inhibits axial electron drifts. Lorentz forces, generated by the interaction of the magnetic field and azimuthal electron Hall currents, couple the thrust to the accelerator structure. Recent experiments indicate that the potential distribution, electron temperatures, and particle densities within the accelerating region plasma are consistent with requirements for proper operation. Thrust and ion current data are obtained with a target thrust balance. Thrust densities of 0.5 mlb/cm² (17.6 mlb in the present laboratory accelerator) have been measured at cesium flow rates equivalent to 3.7 amp and at a specific impulse of 1600 sec. Ion current densities in excess of 100 ma/cm² have been obtained at cesium flow rates approaching the limit of the test facility capabilities. Ion current and cesium flow measurements agree to within the accuracy of the flow metering system, indicating high utilization efficiency. Ion currents of about 50% of the total accelerator current have been measured. Performance trends and criteria for operation at high over-all efficiency are discussed.

Introduction

THE electrostatic acceleration of ions in an annular, low-density, "E-M region" plasma by the interaction of an azimuthal Hall current with a radial magnetic field has been considered[1–3] as a mechanism for the generation of propulsive thrust. A Hall-current accelerator of this type using cesium as a propellant offers the promise of high efficiency and thrust density in the 1500–5000 sec specific-impulse regime at moderate voltages.[4] The acceleration process occurs in a region where the ion space charge is neutralized by the presence of an electron density equal to the ion density. Electron mobility in the axial direction is inhibited by the presence of the radial magnetic field, which is adjusted so that the electron cyclotron radius is small and the ion cyclotron radius is large as compared to the accelerator dimensions. As a result of these conditions, the plasma can support an axial electric field, which provides the ion acceleration mechanism. Thrust is coupled to the magnetic field coil structure by means of a Lorentz force generated by the azimuthal Hall current and the radial magnetic field.

The use of cesium as a propellant is advantageous from the standpoint of ion production, since surface-contact ionization may be employed, or alternately, efficient ionization may be achieved by electron bombardment. In addition, the relatively high atomic weight of cesium permits the use of high magnetic fields without violating the condition $r_i > L$.

In the present accelerator, the specification of low density implies not only that the electron mean free path is large compared to the cyclotron radius ($\omega_e\tau_e \gg 1$) but that it is relatively large as compared to acceleration dimensions. Collisions impede rather than contribute to the acceleration process, and hence neutrals cannot be accelerated. For high over-all efficiency, the propellant must be fully ionized at the entrance to the accelerating region. This feature distinguishes the present apparatus and similar low-density devices[1–3] from annular Hall accelerators of relatively high gas density.[5–7]

The major limitation to the performance of the low-density annular Hall accelerator is the effect of nonclassical (anomalous) transport processes on the magnitude of the axial electron current.[4] The mobility of electrons across field lines resulting from various instability mechanisms can be considerably larger than predicted from classical particle-particle interactions, and such enhanced transport processes have been observed in annular Hall accelerators.[1,8–10] Losses due to axial electron currents may thus be prohibitive from the standpoint of over-all accelerator efficiency. The present state of understanding of such nonclassical loss processes is incomplete, necessitating experimentation whenever a quantitative engineering evaluation of a particular system is required. In Ref. 4, preliminary experiments with an annular Hall accelerator using a surface-contact ionizer and cesium as a propellant are described. These experiments demonstrated that a number of conditions essential to efficient operation were achieved, including the attainment of high ion current densities and high discharge impedance. Means of avoiding losses due to high axial electron currents resulting from the onset of a two-stream instability[8] were outlined. However, a number of problems remained pertaining to the relative contributions of surface and volume ionization processes and to the evaluation of over-all accelerator performance. The work reported in Ref. 4 has been continued in the present investigations, the major objectives being to determine the performance of the existing accelerator directly by means of an over-all thrust measurement and to explore the operation of this accelerator at higher ion current densities and thrust levels with a view toward establishing design criteria for high performance thrustors.

Hall-Current Accelerator Processes

A description of particle trajectories and current flows within the Hall-current accelerator is presented in Fig. 1. The magnetic field is provided by an axisymmetric ferromagnetic core and is essentially radial. An axial electric field E_z is provided by applying a voltage V_a between the anode and a downstream cathode (neutralizer); insulating walls prevent the plasma from shorting through the magnet pole pieces. The predominant electron motion consists of a circular thermal motion about magnetic field lines superimposed on an axial drift $v_{e_{D\theta}}$ in the $\mathbf{E} \times \mathbf{B}$ direction, producing

Presented as Preprint 64-697 at the AIAA Fourth Electric Propulsion Conference, Philadelphia, Pa., August 31–September 2, 1964; revision received December 21, 1964.

* Associate Research Engineer, Electrical Propulsion, Research Laboratories.

† Chief, Electrical Propulsion, Research Laboratories. Associate Fellow Member AIAA.

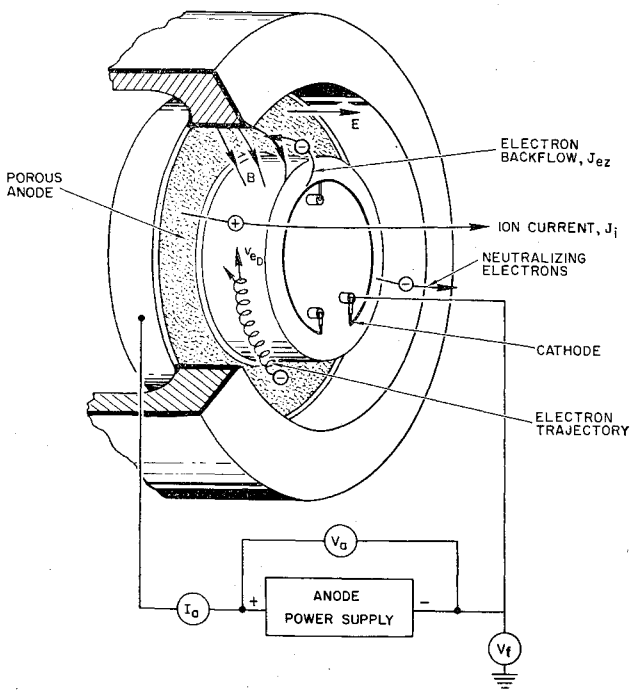

Fig. 1 Currents and particle trajectories in accelerating region.

an azimuthal Hall-current density $J_{e\theta}$. The drift of electrons in the axial direction (v_{ez}) produces an axial current density J_{ez}, which constitutes the major loss in the system. For efficient operation, it is necessary that J_{ez} be less than the ion current density leaving the accelerator J_i. The exiting ion current is neutralized by an equal current of electrons emanating from the cathode as shown in Fig. 1.

The collective motion of the electrons in the accelerating region can be described approximately by a one-dimensional axisymmetric momentum balance when wall interactions and radial gradients are neglected. It has been shown[1,4,5,8] that, under these assumptions,

$$J_{e\theta}/J_{ez} = \omega_e\tau_e \tag{1}$$

where ω_e is the electron cyclotron frequency, and τ_e is the electron momentum-loss collision frequency. Electron mobility across the magnetic field can exceed the rate determined by classical particle-particle interactions as a result of macroscopic or microscopic plasma fluctuations. A large-scale, coherent, azimuthal fluctuation attributable to the onset of a two-stream instability has been observed in an annular Hall-current accelerator,[1, 8] and a criterion for avoiding this instability is presented in Ref. 8. The decay of gross fluctuations to plasma turbulence has been examined in Ref. 10. Measurements of effective diffusion coefficients in an annular Hall accelerator[9] have shown that values of $\omega_e\tau_e$ of approximately three are attainable in an argon plasma. The technique employed in Ref. 9 entails the determination of ion swirl angle in the vicinity of the anode and makes use of the fact that this angle appears in the electron momentum balance. In the present investigation, an "effective" value of $\omega_e\tau_e$ is obtained in an elementary fashion using a similar indirect measurement.

Thrust per unit area of the acceleration is given by

$$\frac{F}{A} = \int_0^L f_z\,dz = \int_0^L J_{e\theta}\,B_r\,dz \tag{2}$$

where f_z denotes the local thrust density. Under the assumption that all ionization occurs at anode potential and that the ion velocity at the exit is essentially axial, Eq. (1) and the condition B_r = const can be used to obtain a relationship between J_i, J_{ez}, and an average value of $\omega_e\tau_e$, since

$$\frac{F}{A} = \frac{m_i n_i v_i^2}{A}\bigg|_{\text{exit}} = \int_0^L J_{ez}\omega_e\tau_e B_r dz$$

$$(m_i v_i/e)(e n_i v_i/A) = J_{ez}B_r\,\overline{(\omega_e\tau_e)}L$$

and, therefore,

$$\overline{(\omega_e\tau_e)} = (r_i/L)(J_i/J_{ez}) \tag{3}$$

where r_i is the ion cyclotron radius at the exit velocity. Equation (3) permits the calculation of representative values of $\omega_e\tau_e$ without inquiring into the details of the transport process. In addition, if the axial electron current is not due to macroscopic fluctuations (i.e., when $\omega_e\tau_e$ is a function of local plasma conditions), Eq. (3) suggests that increasing the accelerator length (within the limitation $r_i \gg L$) will result in a decrease in J_{ez} for a given specific impulse and thrust density. The two-stream instability described in Refs. 1 and 8 should be avoided by using the criterion that the drift velocity not exceed a critical value such that

$$E/B = v_D < v_{D_{cr}} = (kT_i/m_e)^{1/2} \tag{4}$$

where T_i is the ion temperature in a frame of reference moving with the ions. In the experimental work described below, it will be noted that the appearance of low-frequency, large-amplitude oscillations in accelerator current and voltage can be correlated with variations in magnetic field according to the inequality in Eq. (4). Since $E \approx V_a/L$, Eq. (4) leads to the following limitations on accelerator length:

$$V_a/v_{D_{cr}}B < L$$

With the further requirement of large ion cyclotron radius, we have

$$v_i/2v_{D_{cr}} < L/r_i < 1 \tag{5}$$

As an example, an ion temperature of about 0.1 ev and a specific impulse of 3000 sec leads to the following limitation on accelerator length and magnetic field:

$$4500 < BL < 40{,}000 \quad \text{gauss-cm}$$

whereas, for a specific impulse of 1500 sec, we have

$$1120 < BL < 20{,}000 \quad \text{gauss-cm}$$

In the experiments reported below, L = 2.5 cm, and at a specific impulse, typically of 1500 sec, the lower limit on the value of magnetic field for avoiding the onset of two-stream instabilities was about 450 gauss.

It is significant to note from Eq. (5) that

$$(I_{sp}/27{,}000)(0.1/T_i)^{1/2} \ll 1$$

where T_i is in electron volts, and hence, as specific impulse increases, it becomes increasingly difficult to avoid incurring

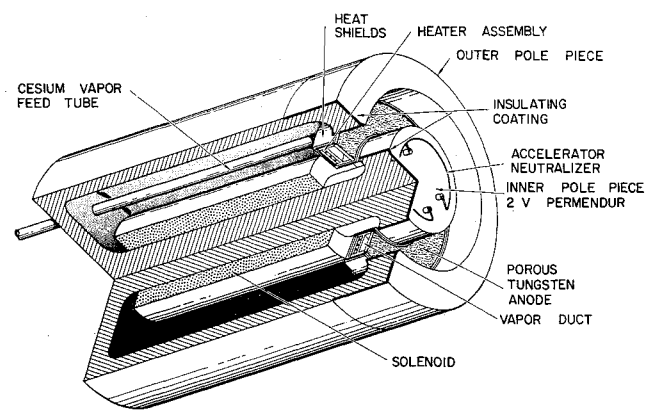

Fig. 2 Experimental accelerator.

losses due to ion swirl and at the same time avoid losses due to the appearance of the two-stream instability. A specific impulse of about 7000 sec appears to be the upper limit for efficient operation of this type of Hall accelerator; this specification is independent of thrust density, magnetic field strength, accelerator length, and ion mass, and only weakly dependent on ion temperature.[4]

An additional requirement for efficient accelerator performance is that ionization of the propellant be complete in the vicinity of the anode. For surface-contact ionization, this condition is met at low ion current densities; however, at higher mass flow rates, it is necessary for volume ionization of the ionizer neutral efflux to occur. In a gas-discharge accelerator, it is essential that nearly complete ionization occur in the plasma adjacent to the anode, so that all ions are accelerated through the full applied voltage. It is desirable, therefore, to introduce the propellant into this region directly. One means of accomplishing this is through a porous anode, implying that the annular porous-wall apparatus shown in Fig. 2 is well suited for use as a propellant distribution system in a gas-discharge Hall accelerator. The use of alkali metals in this connection is particularly attractive because of their high-ionization cross sections and low-ionization potentials. In the present experiments, the ionization mean free path of a neutral on leaving the anode was at all times less than 1% of the accelerator length.

Analyses of the Hall-current accelerator used with a surface-contact ion source,[4] have shown that efficient performance can be achieved if the power loss due to electron backflow is dissipated at the ionizer surface, i.e., if the electron backflow is essentially adiabatic. Electron-electron interactions contribute to rapid thermalization to some local electron temperature determined (in the adiabatic limit) by the local potential. However, collisions of electrons with the annulus walls represents an undesirable dissipative process. As a result of the high mobility of electrons in the radial direction, such collisions may be significant depending upon the value of the wall secondary emission coefficient. For a coefficient less than one, a wall potential sheath will form to preserve ion and electron current neutrality, and the electron current to the wall will equal the ion current. However, for cases in which the secondary emission coefficient exceeds 1.0 over some range of incident electron energy, the electron current to the wall will exceed the ion current, and high-energy primary electrons drawn from the plasma will be continually replaced by low-energy secondary electrons. As a result, the local electron temperature will be less than the value predicted from adiabatic considerations. Since the local plasma density is determined by the ion density, and hence by the local plasma potential, wall interactions will affect the acceleration process only indirectly. This might occur, for example, if electron mobility in the presence of microscopic fluctuations were temperature-dependent, resulting in significant changes in the axial potential distribution. The performance of a surface-contact Hall accelerator is thus more sensitive to wall effects than that of a gas-discharge accelerator, since the latter does not require dissipation of the backflow loss at the anode. With volume ionization, it is only necessary that the electron temperature and density in the vicinity of the anode be sufficiently high to provide complete ionization close to the anode. If this condition exists, then the ion exhaust velocity of a gas-discharge accelerator will be uniform, eliminating its principal disadvantage in comparison with the surface-contact accelerator. Furthermore, the ion current density and hence thrust density of the gas-discharge device is limited primarily by the condition that $\omega_e\tau_e \gg 1$. Ionizer emission considerations place an additional constraint on achievable current density in the surface-contact accelerator. The foregoing factors suggest that the low-density cesium Hall-current accelerator will be more efficient using volume ion production rather than surface production. The experiments reported below substantiate this argument in that, after having been generated by electron impact, ions appear to leave the accelerating region at the full value of net accelerating potential, $V_n = V_a - V_f - V_s$, where V_f is the cathode floating potential, and V_s is the target sheath potential (see Fig. 3).

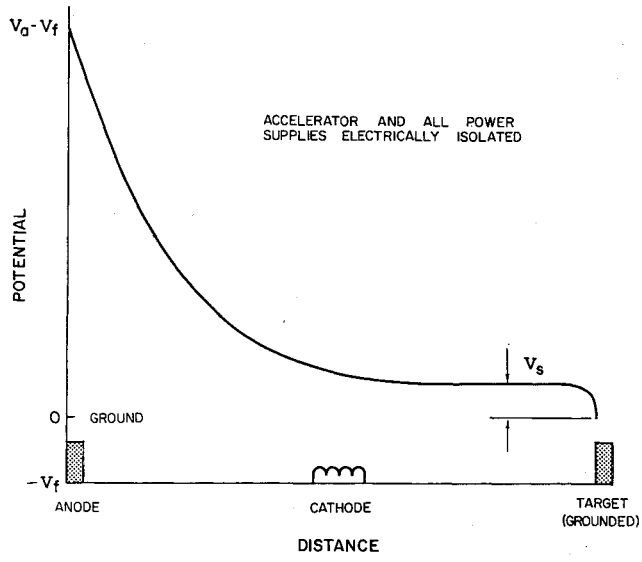

Fig. 3 Axial plasma potential distribution.

Experimental Apparatus

The experimental evaluation of the cesium Hall-current accelerator described in Ref. 4 was continued in the present program with only minor modifications to the accelerator and feed system apparatus. The major addition to the existing test equipment was the installation of a target thrust balance.

Accelerator Design

The experimental annular Hall-current accelerator is shown schematically in Fig. 2. The existing solenoid and core can generate a radial magnetic field of up to 3000 gauss in the 2.2 cm annular gap between inner and outer pole pieces. An insulating coating consisting of flame-sprayed alumina is used to prevent the pole pieces from short-circuiting the plasma. The axial electric field is produced between the anode and a thermionic cathode. The cathode consists of a directly heated, lanthanum-hexaboride-coated, tantalum filament located 2.5 cm downstream of the anode.

Cesium propellant is introduced into the accelerating region through a porous tungsten anode having a mean diameter of 8.9 cm and a frontal area of 35.5 cm^2. A heater consisting of 0.030 in. rhenium wire, insulated and supported by high density, high-purity alumina, is used to heat the anode surface. Tantalum heat shields are provided as shown in Fig. to reduce the radiant power losses.

Cesium Feed System

Cesium vapor is transported to the anode through a molybdenum tube from a feed system consisting of an electrically heated boiler, an orifice plate, a hand-operated shutoff valve and a purging and refill system. All components of the feed system are heated to avoid cesium condensation. The boiler is operated under saturated vapor conditions.

Calibration of the feed system is accomplished by the flow depletion method. A time-average mass flow rate $\langle \dot{m} \rangle$ is obtained by bringing the boiler up to operating temperature, charging the boiler with a known amount of cesium, and allowing the accelerator to run until the cesium is depleted

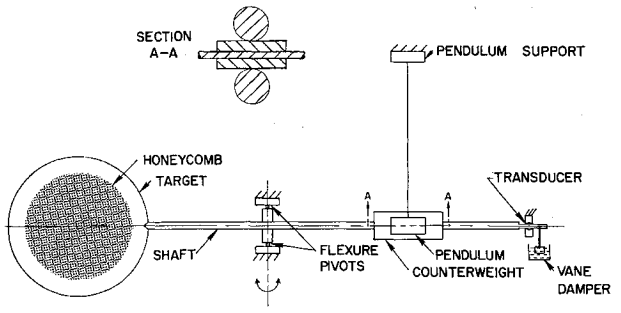

Fig. 4. Target thrust balance.

To correct for variations in flow rate during starting and stopping, a calibration run at fixed accelerating potential is made at a particular boiler temperature, during which time target thrust is recorded as a function of time. At the higher voltages, curves of F vs $V_n^{1/2}$ indicate that utilization efficiency is constant, and hence mass flow will vary linearly with thrust, permitting a first-order correction to be made to $\langle \dot{m} \rangle$. At a boiler temperature corresponding to the highest flow rate used in the present experiments, the difference between the maximum mass flow during a given run $\dot{m}_{\max}$ and $\langle \dot{m} \rangle$ is about 30%. This figure is reduced at lower flow rates because of the longer run times available.

Target Thrust Balance

Accelerator thrust is measured by the simple target thrust balance shown schematically in Fig. 4. A photograph of the balance assembly is shown in Fig. 5. The exhaust beam impinges on an 8-in.-diam honeycomb-faced copper target. The target is connected to a shaft 22 in. long, which rotates in the horizontal plane around a pair of flexure pivots located 11 in. from the center of the target.

Shaft displacement is measured by a transducer consisting of a d.c. differential transformer. The output signal is recorded on a four-channel recorder in time sequence with the applied voltage V_a and the total current I_a.

A pair of cylindrical pendulum bobs rests against the shaft counterweight and provides restoring forces to the shaft. With these pendulums, it is possible to null the target at a known position. The pendulums were designed to give a spring constant for the system corresponding to a target thrust of 20 mlb at maximum displacement. A vane-type viscous damper (Fig. 4) was added to the balance to give a nearly critically damped response to a thrust step function input.

Calibration of the balance to a repeatability of 3% was performed both by dead loading with standard weights and by computing the spring constants of the pendulum system.

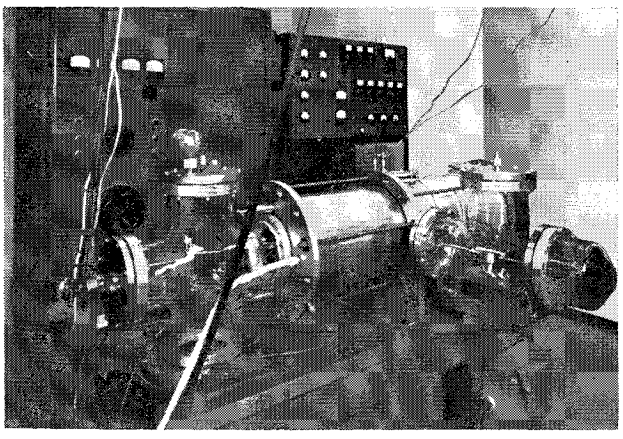

Fig. 5 Vacuum facility and thrust balance.

Appropriate corrections were made, where possible, for misalignment between the beam and the center of the target, by observation of sputtering patterns. No attempt was made to compensate for the effects of possible azimuthal asymmetries or for portions of the exit beam missing the target, although these effects on the over-all thrust measurement are believed to be small. Comparisons of cesium flow rates with target weight losses due to sputtering show that any error due to the reaction from sputtered or vaporized material is negligible.

Vacuum Facility

The experiments were conducted in the 12-in.-diam vacuum chamber shown in Fig. 5. The glass section shown in Fig. 5 extending perpendicular from the main vacuum chamber enclosed the thrust balance assembly. The target is located at the center of the large flange shown between two 12-in. sections of the vacuum chamber. Electrical isolation was provided for all power supplies so that the accelerator could be operated in a grounded or floating condition. Probe measurements were obtained with a traversing axial Langmuir probe.

The pumping system consists of an LN_2-cooled cesium condenser and a water-baffled 4-in. oil diffusion pump. Ambient pressure levels below 10^{-5} mm Hg can be obtained at low mass flow rates (less than 1 amp of equivalent ion current). However, because preliminary tests indicated performance increases with mass flow, the majority of the experiments reported herein were conducted at $I_m > 3$ amp. As a result of these high cesium flow rates and the increased blockage caused by the installation of the thrust target, cesium condensation on the external accelerator structure and leads introduced breakdown problems. At a particular mass flow, there generally exists some upper limit to V_a for which breakdown occurs (depending somewhat on the length of the run). This limit decreases with increased mass flow and increased run duration. Tests in the high mass flow regime reported herein were limited by the facility pumping capacity to specific impulses below 1600 sec. Even at these conditions, some leakage currents were observed. Exploration of the full potentialities of the cesium Hall-current accelerator will require an engine-mounted thrust balance and a facility capable of handling cesium flow rates of about 10 amp at pressures below 10^{-5} mm Hg.

Discussion of Experimental Results

Preliminary experiments with a cesium Hall-current accelerator[4] raised a number of questions regarding the po-

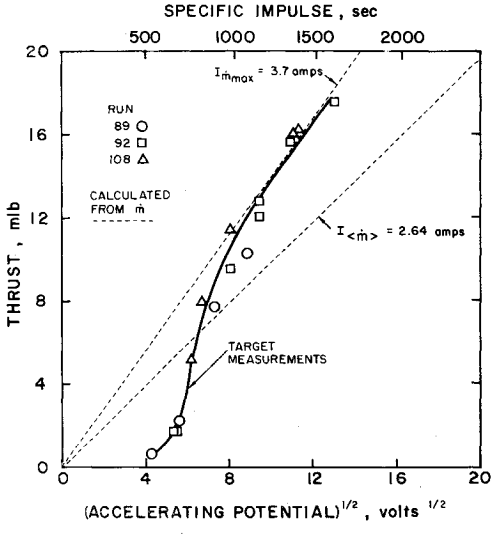

Fig. 6 Measured thrust compared to theoretical thrust at measured mass flow.

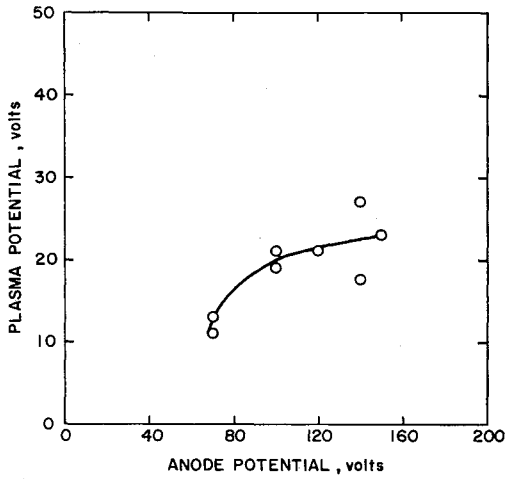

Fig. 7 Plasma potential in vicinity of cathode.

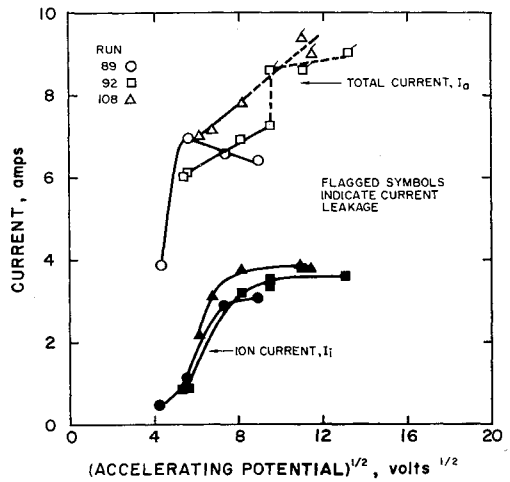

Fig. 8 Variation of total current and ion current with net accelerating voltage.

tentialities of the device in terms of thrust, efficiency, electron backflow, and relative contribution of surface and volume ionization processes. The experiments conducted during the present investigation were designed to provide answers to these questions. Results of the early work indicated that, at a particular mass flow, there exists a limiting magnetic field, beyond which a discharge cannot be maintained. This limiting field increases with increasing mass flow. At low mass flows, drift velocities corresponding to these limiting fields are generally above the critical value of Eq. (4) for specific impulses of interest. Accordingly, in the present investigation, efforts were concentrated on operating at high mass flows ($\dot{m} > 3$ amp) and high magnetic fields ($B > 400$ gauss).

In starting a run, the cesium feed system, the porous anode, and the cathode are first brought up to operating temperature. Cesium is then introduced into the boiler and the shutoff valve is opened to admit vaporized cesium into the anode. The magnetic field solenoid current and anode voltage V_a are then applied and adjusted to the desired value. All appropriate currents, voltages, and temperatures are monitored. In general, the target is grounded to the vacuum chamber whereas the cathode is allowed to float electrically at a potential V_f, as shown in Figs. 1 and 3.

To determine the net accelerating potential V_n, it is necessary to monitor the exit plasma potential (see Fig. 3) since, in the test stand, a sheath having a potential drop V_s can form between the exhaust beam plasma and the target. The cathode sheath potential $V_f + V_s$ cannot be neglected in evaluating performance at low accelerating voltages. In the present experiments, measurements of plasma potential in the cathode plane were obtained by conventional Langmuir probe techniques.

Thrust

The maximum thrust measured to date is 17.6 mlb at a specific impulse of 1600 sec, corresponding to a thrust density of about 0.5 mlb/cm^2 of anode area. As mentioned previously, these values are limited only by the size of the present feed system and the pumping capacity of the present test facility.

The measured target thrust obtained at a boiler temperature corresponding to a cesium flow rate of 3.7 amp is presented in Fig. 6 as a function of $V_n^{1/2}$. Since the low-density Hall-current device behaves as an electrostatic ion accelerator, the usual ideal relationship between thrust, ion current, and accelerating voltage holds, which for cesium ions is

$$F = 0.375\, I_i V_n^{1/2} \quad \text{mlb} \tag{6}$$

Two lines are shown in Fig. 6 representing the theoretical thrust corresponding to complete ionization of the cesium propellant. The lower value corresponds to $I_{\langle \dot{m} \rangle} = 2.64$ amp, the propellant consumption averaged over the entire run, whereas the upper value corresponds to the maximum equilibrium rate of 3.7 amp calculated by the correction procedure noted previously. The measured thrust data approach this line asymptotically at accelerating voltages above 100 v within the experimental accuracy of the feed system, indicating essentially complete ionization of the propellant at anode potential.

The variation of plasma potential (relative to the cathode) at a point taken at the mean annulus radius in the plane of the cathode is presented in Fig. 7 as a function of applied anode potential V_a. As V_a increases, the plasma potential approaches a limit of perhaps 25 v. Thus, as specific impulse increases, the magnitude of the loss due to the presence of the cathode sheath $(V_f + V_s)I_a$ decreases relative to the accelerator power $P_a = V_a I_a$.

The anode temperature corresponding to the data points shown in Fig. 6 was appreciably below the temperature necessary to account for the ion current densities achieved at the higher thrust levels (~100 ma/cm^2) by surface-contact ionization. The predominant ionization mechanism under these circumstances is electron bombardment. For operation at high utilization efficiency and uniform exhaust beam conditions, it is thus necessary that electron energies in the vicinity of the anode be large relative to the ionization potential, implying that there exists some lower limit on applied voltage below which efficiency and thrust would be expected to drop rapidly. This limit corresponds approximately to $V_a \approx 70$ v as shown in Fig. 6 (and applying the correction for plasma potential of Fig. 7).

From the data shown in Figs. 6 and 7, it appears as if efficient performance, from the standpoint of propellant utilization, beam uniformity, and cathode sheath losses, may be expected from the cesium Hall-current accelerator at specific impulses of about 1500 sec and above.

Ion Current

Measured thrust and accelerating potential data can be used in conjunction with Eq. (6) to determine the ion current issuing from the accelerator under the assumption (conservative insofar as the calculation of ion current is concerned) that all ions emerge in the axial direction at an energy eV_n. Values of ion current computed for the thrust data of Fig. 6 are presented in Fig. 8. As the accelerating potential increases, the calculated ion current approaches a saturation limit corresponding to the mass flow emanating from the anode. The spread in this saturation value for the data shown in Fig. 8 is indicative of the repeatability of the present feed

system when adjusted to the same boiler temperature after refilling.

In an experiment to determine the contribution of surface-contact ionization to the ion current, several runs were made during which the anode (ionizer) temperature was varied between 900° and 1500°K. At the higher temperature, thrust was observed to vary by a small amount corresponding to anticipated surface ion emission rates provided the accelerating voltage was below 70 v. At the higher voltages, essentially complete ionization was achieved regardless of anode temperature. At temperatures below about 1000°K, changes in anode conductance to cesium vapor caused appreciable reductions in mass flow and thrust, eventually extinguishing the discharge at 900°K.

Electron Backflow

Measurements of total current I_a corresponding to the preceding ion current data are also presented in Fig. 8. Run 89 is typical of anode current behavior at low mass flows, i.e., I_a peaks at some intermediate voltage and drops slowly with further increases in voltage. However, at the slightly higher mass flows of runs 92 and 108 (as evidenced by the somewhat higher ion current asymptotes), electrical breakdown and leakage currents were observed at a number of locations. Data points for which visual evidence of such leakage was obtained are denoted by flagged symbols in Fig. 8. Local arcs between the cathode and porous sections of the insulating walls were observed and apparently were the predominant cause of increased I_a, with some additional contributions due to leakage across standoffs that had been exposed to target sputtering or cesium condensation. Attempts to operate the accelerator at increased anode voltages and specific impulses at these high mass flow rates were accompanied by pronounced arcing and large increases in leakage currents with subsequent deterioration of insulator and accelerator structure.

The ratio of ion current to total current is presented in Fig. 9 showing an increase with V_a to a maximum of about 48% in the absence of leakage, corresponding to $J_i/J_{ez} = 0.92$. Measurements of ion current and electron backflow by the thrust target technique at lower mass flows (to avoid the current leakage problem) indicate that ion current ratio increases both with increasing mass flow and increasing specific impulse.

Calculations using Eq. (3) and the data obtained at specific impulses in excess of 1000 sec (for $I_m = 3.7$ amp) indicate that representative values of electric field and $\overline{\omega_e\tau_e}$ are 50 v/cm and 7, respectively. For these high mass flow conditions, the magnetic field (optimized for maximum thrust) was set at approximately 1100 gauss, and the plasma was relatively quiescent. Oscilloscope traces of V_a and I_a show noise up to 200 kc with a maximum amplitude less than 10% of the d.c. value. Varying the magnetic field between 400 and 1200 gauss produces only small changes in thrust and essentially no change in fluctuation amplitude. Below about 400 gauss, a coherent, large-amplitude fluctuation at a frequency of the order of 10–20 kc appears in both V_a and I_a. The onset of these fluctuations is accompanied by large increases in I_a and decreases in thrust. As noted in the previous section, at $I_{sp} = 1500$ sec in the present accelerator, 450 gauss appears to be a lower limit for avoiding the onset of the streaming instability of Ref. 8. Although the accelerating region plasma was not instrumented to observe the character of the fluctuation, the observed frequency corresponds rather well with the frequencies of about 50 kc observed in Ref. 8 for fluctuations due to a two-stream instability in an annular argon plasma, considering the differences in annulus diameter and ion mass (which effects the speed of the azimuthal space-charge wave).

The foregoing results indicate that microscopic fluctuations are the primary cause of electron backflow, provided that

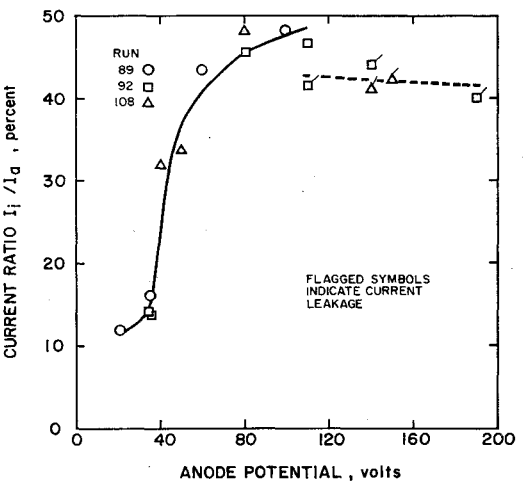

Fig. 9 Ratio of ion current to total current.

B is made sufficiently large according to Eq. (4). Although $\overline{\omega_e\tau_e}$ is appreciably lower than would be expected for classical electron transport, the effective value of about 7 obtained at electric fields of 50 v/cm shows that, according to Eq. (3), if accelerator length is increased (by say a factor of 2), J_i/J_{ez} can be increased significantly. Sufficient latitude exists for such increases in L without incurring excessive losses due to ion swirl.

Measurements of anode temperature indicate that at high $\dot{m}$ only about one-third of the energy loss due to electron backflow is dissipated at the anode. This result differs somewhat from plasma potential and electron temperature data, obtained in axial probe traverses through the accelerating region during operation at low $\dot{m}$, which indicate that the electron backflow is adiabatic. Probe data could not be obtained in the present series of tests at high $\dot{m}$ because of rapid probe deterioration and significant interference of the probe with the over-all discharge characteristics.

Neutralization

The performance data presented in Figs. 6–10 were obtained with the cathode (neutralizer) heated to a temperature such that emission was limited by external conditions. Increasing cathode temperature beyond this point has essentially no effect on accelerator operation. However, decreasing the temperature to the point where the cathode operates under emission-limited conditions results in large decreases in thrust and increases in the cathode sheath potential $V_f + V_s$. In this respect, the behavior of the low-density Hall-current accelerator resembles that of any isolated electrostatic thrustor. The presence of cathode electrons is essential for proper thrust generation; in the present case, electrons are required for space-charge neutralization in the accelerating region as well as in the exhaust beam.

Langmuir probe measurements of electron density and plasma potential in the vicinity of the cathode show that n_e agrees with n_i to within a factor of 3 when n_i is computed from the measured ion current, the local potential, and an assumed beam area. This agreement is well within experimental accuracy.

As a result of the presence of electron backflow, an upper limit to the efficiency of the present Hall-current accelerator is

$$\eta_{max} < I_i/I_a \approx 1/(1 + J_{ez}/J_i)$$

When other losses encountered in the acceleration processes are included (i.e., ion interception at the wall, excitation and ionization losses, cathode sheath losses, nonuniform exit velocity, neutral efflux, ions wirl, ion heating, etc.), we have

$$\eta = F^2/2\dot{m}V_aI_a < I_i/I_a \qquad (7)$$

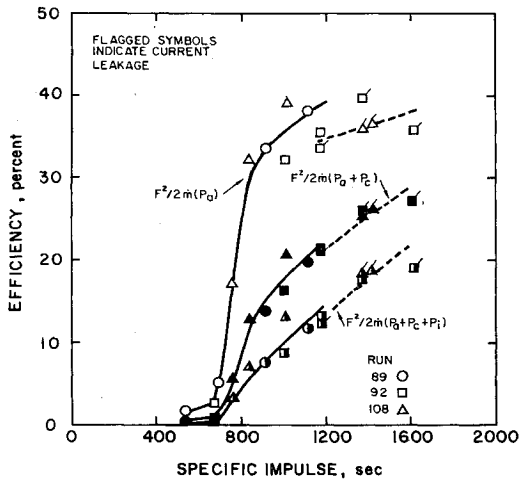

Fig. 10 Variation of over-all efficiency with specific impulse.

Values of current ratio presented in Fig. 9 are somewhat conservative in that the use of a thrust measurement to compute I_i does not account for the effects of nonaxial or nonuniform ion exit velocities. However, the efficiency as computed from Eq. (7) is a meaningful indication of acceleration region performance for electrical propulsion purposes. Values of $F^2/2\dot{m}P_a$ are presented in Fig. 10 for the tests described previously. The maximum efficiency obtained to date is 40%, and the trend clearly shows an increase in η with I_{sp}. The effects of current leakage are also noted, having caused about a 10% decrease in η. The primary reason for the difference in η and I_i/I_a is the loss due to the cathode sheath potential drop (Fig. 3). As shown in Fig. 7, this drop approaches a constant value with increasing V_a, and hence, for further increases in I_{sp}, the efficiency would approach I_i/I_a.

The major parasitic loss in the gas-discharge accelerator is the cathode heating power P_c (neglecting magnetic field generation requirements under the assumption that these will be small, or that the field can be produced by permanent magnets). The lanthanum-hexaboride cathode used in the present test series was selected because of its ease of manufacture, simple activation procedure, and tolerance to contamination and ion bombardment. Although it is a rather inefficient cathode from the standpoint of input power requirements, efficiency has also been computed from

$$\eta = F^2/2\dot{m}(P_a + P_c) \tag{8}$$

and is presented in Fig. 10 to present a more complete picture of the effects of parasitic losses. As specific impulse increases, the effect of P_c on efficiency decreases, as evidenced by the manner in which the curves of Fig. 10 converge.

Although surface-contact ionization was not the principal source of ion current, it is of interest to exhibit the effect of ionizer heater power input P_i on efficiency in the present experiments, where now

$$\eta = F^2/2\dot{m}(P_a + P_c + P_i) \tag{9}$$

Data are presented in Fig. 10 showing the reduction in efficiency due to ionizer input power. As noted previously, essentially no change in performance was obtained when the temperature was lowered to about 1000°K, at which point the reduction of η due to P_i is only a few percentage points at $I_{sp} \approx 1500$ sec.

Conclusions

1) Experiments with the first annular Hall-current accelerator designed for use with cesium have demonstrated thrust levels of 17.6 mlb and thrust densities of 0.5 mlb/cm^2 at a specific impulse of 1600 sec with complete volume ionization. Over-all efficiencies of 40% have been achieved in the present research apparatus, exclusive of neutralizer and feed system power.

2) Electron backflow, which is the major source of loss in the annular Hall-current accelerator, was observed at about 52% of the total accelerator current at the higher mass flows and specific impulses.

3) Thrust increases linearly with mass flow in the range of 100 ma/cm^2 of ion current. At this current density and at $I_{sp} \approx 1500$ sec, further increases in ion current and particle density cause no apparent reduction in performance due to increased electron collision frequency.

4) Essentially complete ionization and uniform ion exhaust velocity can be achieved with volume ionization of cesium. Under these conditions, the use of surface-contact ionization and its attendant reduction in over-all efficiency due to ionizer heater power requirements is not warranted. With volume ionization, dissipation of electron backflow power at the anode is not required, allowing a greater latitude in the specification of the insulating wall structure.

5) The length of the accelerating region should be made as large as possible, consistent with the requirement $r_i/L \gg 1$. Decreases in electron backflow with accompanying increases in efficiency beyond those values presently achieved are possible with increased length.

6) Enhanced electron transport due to microscopic fluctuations in a fully ionized, $n > 10^{11}$/cm^3, cesium plasma occurs in the present Hall-current accelerator at an "effective" $\omega_e\tau_e$ of 7 for cesium mass flows in the neighborhood of 100 ma/cm^2. This value has been observed to increase with increasing mass flow and specific impulse. The two-stream instability criterion of Ref. 8 appears to hold in the present environment. Advanced accelerator designs can employ these results in reducing electron backflow losses.

References

[1] Lary, E. C., Meyerand, R. G., Jr., and Salz, F., "Ion acceleration in a gyro-dominated neutral plasma—theory and experiment," Bull. Am. Phys. Soc. **7**, 441 (1962).

[2] Seikel, G. R. and Reshotko, E., "Hall-current ion accelerator," Bull. Am. Phys. Soc. **7**, 414 (1962).

[3] Janes, G. S., Dotson, J., and Wilson, T., "Electrostatic acceleration of neutral plasmas—momentum transfer through magnetic fields," *Proceedings of the Third Symposium on Advanced Propulsion Concepts* (Gordon and Breach Science Publishers, Inc., New York, 1963), pp. 153–175.

[4] Pinsley, E. A., Brown, C. O., and Banas, C. M., "Hall-current accelerator utilizing surface contact ionization," J. Spacecraft Rockets **1**, 525–531 (1964).

[5] Hess, R. V., "Fundamentals of plasma interaction with electric and magnetic fields," NASA SP-25, pp. 9–32 (1963).

[6] Cann, G. L. and Marlotte, G. L., "Hall current plasma accelerator," AIAA J. **2**, 1234–1241 (1964).

[7] Powers, W. E. and Patrick, R. M., "Magnetic annular arc," Phys. Fluids **5**, 1196–1206 (1962).

[8] Lary, E. C., Meyerand, R. G., Jr., and Salz, F., "Fluctuations in a gyro-dominated plasma," *Comptes Rendus de la VI^e Conférence Internationale sur les Phénomènes d'Ionisation dans les Gaz* (SERMA, Paris, 1963), Vol. II, Sec. VC, pp. 441–449.

[9] Janes, G. S. and Dotson, J., "Experimental studies of oscillations and accompanying anomalous electron diffusion occurring in d. c. low density Hall type crossed field plasma accelerators," *Proceedings of the Fifth Symposium on the Engineering Aspects of Magnetohydrodynamics* (Massachusetts Institute of Technology, Cambridge, Mass., 1964), pp. 135–148.

[10] Hess, R. V., Burlock, J., Sidney, B., and Brockman, P., "Study of instabilities and transition to turbulence in a linear Hall accelerator," *Proceedings of the Fifth Symposium on the Engineering Aspects of Magnetohydrodynamics* (Massachusetts Institute of Technology, Cambridge, Mass., 1964), pp. 173–174.